

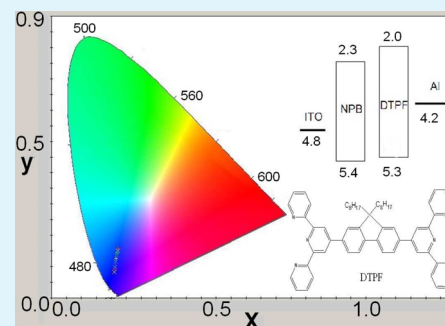
# A Deep-Blue Emitter with Electron Transporting Property to Improve Charge Balance for Organic Light-Emitting Device

Xing Xing,<sup>§</sup> Lipei Zhang,<sup>§</sup> Rui Liu,<sup>¥</sup> Suyue Li,<sup>¥</sup> Bo Qu,<sup>§</sup> Zhijian Chen,<sup>§</sup> Wenfang Sun,<sup>\*,¥</sup> Lixin Xiao,<sup>\*,§</sup> and Qihuang Gong<sup>\*,§</sup>

<sup>§</sup>State Key Laboratory for Mesoscopic Physics and Department of Physics, Peking University, Beijing 100871, P. R. China

<sup>¥</sup>Department of Chemistry and Biochemistry, North Dakota State University, Fargo, North Dakota 58108-6050, United States

**ABSTRACT:** Highly efficient deep-blue organic light-emitting devices (OLEDs) have been fabricated using 2,7-di(2,2':6',2''-terpyridin-4-yl)-9,9-dioctyl-9H-fluorene (DTPF) as the emitter, which has a wide energy gap, high emission quantum yield ( $\Phi_f = 0.88$ ), and high electron transporting property to improve the charge balance. A high efficiency of 2.55 cd/A and 2.67 lm/W are obtained in OLED. The device also exhibits a low turn-on voltage of 3.0 V and Commission Internationale de l'Éclairage (CIE) coordinates of (0.16, 0.09).



**KEYWORDS:** organic light-emitting device, deep-blue, electron transport, charge balance, emitter

## INTRODUCTION

Organic light-emitting devices (OLEDs) have been commercialized for applications in displays and solid state lightings because of the success of developments in materials during the past few decades.<sup>1–4</sup> Up to date, red and green emitters primarily match the requirements of application on color purity, lifetime and efficiency.<sup>5–8</sup> The development of highly efficient deep-blue emitters for full color OLED applications is still on the way.

According to the National Television Standards Committee (NTSC), standard blue is required to be at Commission Internationale de l'Éclairage (CIE) coordinates of (0.14, 0.08). Therefore, it is highly desirable to develop efficient deep-blue emitters with CIE<sub>y</sub> < 0.10. However, although tremendous efforts have been paid to the development of deep-blue emitters, most of them give a light ranging within CIE ( $x < 0.15$ ,  $y < 0.15$ ).<sup>9,10</sup> For the development of color saturated displays, a saturated deep-blue emitter with CIE<sub>y</sub> < 0.10 and high efficiency is in critical need.<sup>11–14</sup> Wong et al. reported saturated deep-blue OLEDs made from diphenylamino and triphenylamino end-capped oligofluorenes as dopant emitters with maximum efficiencies up to 2.9 cd/A at 2 mA/cm<sup>2</sup> (external quantum efficiency of 4.1%) and CIE coordinates of (0.152, 0.08).<sup>12</sup> However, the turn-on-voltages (~7 V) for these OLEDs are relatively high and the power efficiencies (0.8–1.24 lm/W) are moderate.<sup>12</sup> Very recently, Cho et al. also reported a saturated deep-blue emitter of 9-(9-phenylcarbazole-3-yl)-10-(naphthalene-1-yl)anthracene (PCAN) at CIE (0.151, 0.086) with a  $\eta_{ex}$  of 4.61%, but a relatively high turn-on-voltage of 4.6 V and a moderate power efficiency ( $\eta_p$ ) of 1.41 lm/W.<sup>13</sup> Kwon et al. reported a pure blue emitter with a CIE coordinate of (0.14, 0.08) from 9,10-bis[(2'',7''-di-*t*-butyl)-9',9'-

spirobifluorenyl]anthracene (TBSA). However, the  $\eta_p$  (0.54 lm/W) still needs to be improved.<sup>14</sup>

Generally, the hole mobility is much higher (about 1000 times) than the electron mobility in organic semiconducting materials,<sup>15</sup> and thus holes are much easier to transport than electrons in OLEDs. Moreover, in the case of deep-blue emitters with wide energy gap ( $E_g$ ), it is more essential to enhance the electron transporting properties of emitters to improve charge balance for achieving higher efficiency. This is because wide  $E_g$  indicates weak conjugation of the molecule, which could lead to a low electron transporting property. To date, only a few emitters with electron transporting property have been reported.<sup>16–18</sup> Recently, Peng et al. reported an electron transporting beryllium complex, bis(2-(2-hydroxyphenyl)-4-methyl-pyridine)beryllium (Be(4-mpp)<sub>2</sub>), with a saturated deep-blue emission at CIE (0.14, 0.09). However, its emission quantum yield ( $\Phi = 0.37$ ) is quite low, although a  $\eta_{ex}$  of 5.4% was obtained.<sup>17</sup>

To remedy the deficiency of currently reported blue emitters, in this letter we report a new blue emitter, 2,7-di(2,2':6',2''-terpyridin-4-yl)-9,9-dioctyl-9H-fluorene (DTPF),<sup>19</sup> which exhibits a high fluorescence quantum yield ( $\Phi_f$ ) of 0.88 at  $\lambda_{max} = 374$  nm, and shows promising as an electron transporting moiety in OLED. Both properties significantly improve the deep-blue emission efficiency for OLED.

Received: April 18, 2012

Accepted: June 7, 2012

Published: June 7, 2012

## EXPERIMENTAL SECTION

The synthesis and characterization of DTPF were reported by Sun's group previously.<sup>19</sup> The samples used for the fabrication of OLEDs passed the elemental analysis. OLEDs were fabricated by the method described in our previous report.<sup>20</sup> The ITO/glass substrate was cleaned by ultrasonication in deionized water, acetone, and ethanol for 20 min prior to device fabrication. All organic materials were then deposited by thermal evaporation under high vacuum ( $8 \times 10^{-4}$  Pa) at a rate of 0.1 nm/s. After the deposition of the organic layers, an ultrathin layer of LiF (1.0 nm) and an aluminum layer (100 nm) were evaporated in vacuum as the cathode, the area of which was defined as the active area of the devices by a shadow mask with 2 mm diameter opening. The thickness of the evaporating layer was monitored with a quartz crystal microbalance. The device performances were measured with a Keithley 2611 source meter and a spectrophotometer (Photo Research 650). All the measurements were carried out in ambient atmosphere at room temperature.

## RESULTS AND DISCUSSION

To investigate the possibility of electron transporting property of DTPF, its conformation and electron density distribution of the highest occupied molecular orbital (HOMO) and the lowest unoccupied molecular orbital (LUMO) were subjected to density functional theory (DFT) optimizations using the B3LYP functional with the 3-21G basis set in Gaussian 09w. It needs to be noted that the long alkyl chains on DTPF were substituted by methyl groups in order to shorten computation time. The calculation results show that the favored conformation for DTPF is nearly planar, which is beneficial to electron transport. The electron density distributions of HOMO and LUMO of DTPF are shown in Figure 1c, d, in

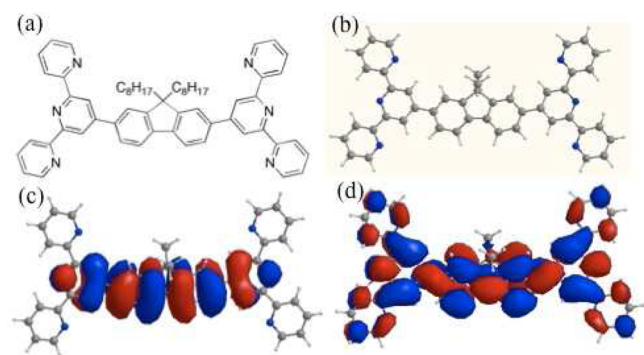


**Figure 1.** (a) Chemical structure of DTPF, (b) optimized conformation of DTPF, (c) electron density of HOMO and (d) LUMO of DTPF, computed by DFT.

which the electron density of the LUMO is delocalized on the whole molecule including the pyridine rings, suggesting that the incorporation of the pyridine unit effectively increase the electron transporting property.

The HOMO level of DTPF is 5.3 eV measured by an Atmosphere Ultraviolet Photoelectron Spectrometer AC-2 (Riken Keiki). The energy gap ( $E_g$ ) between HOMO and LUMO is calculated to be 3.3 eV from the absorption edge of its UV-Vis spectrum in CH<sub>2</sub>Cl<sub>2</sub>.<sup>19</sup> Thus the LUMO level of DTPF can be figured out as 2.0 eV. It is obvious that both the computational and experimental results testify the electron transporting and deep-blue emission properties of DTPF.

To optimize the OLED device performance that uses DTPF as the emitting layer, three devices were fabricated as the following:

- Device I ITO/NPB (50 nm)/DTPF (60 nm)/LiF (1 nm)/Al (100 nm);
- Device II ITO/NPB (50 nm)/DTPF (30 nm)/TPBI (30 nm)/LiF (1 nm)/Al (100 nm);
- Device III ITO/NPB (50 nm)/DTPF (30 nm)/TPBI:PBD (2:1 wt.) (30 nm) /LiF (1 nm)/Al (100 nm).

In Device I, 4,4'-bis[*N*-(1-naphthyl)-*N*-phenyl-amino]-biphenyl (NPB) was used as the hole transporting layer (HTL), and DTPF as both emitting material layer (EML) and the electron transporting layer (ETL). In Devices II and III, 1,3,5-tris(*N*-phenylbenzimidazol-2-yl)-benzene (TPBI) and TPBI:2-*tert*-butylphenyl-5-biphenyl-1,3,4-oxadiazole (PBD) (2:1 by weight) were used as the ETL to replace DTPF, respectively. The structures of the materials used in the devices and their energy levels are given in Figure 2.

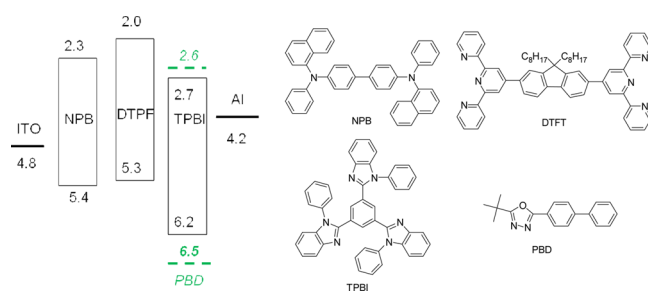


**Figure 2.** Chemical structures and energy levels of materials used in the OLEDs.

Figure 3 shows the current density and luminance vs voltage characteristics of the DTPF based OLEDs. The current density of Device I is the highest, and the maximum luminance of Device I reaches 1300 cd/m<sup>2</sup> at 7.0 V with a low turn-on voltage of 3.5 V, which could be mainly attributed to the excellent electron transporting ability of DTPF. To improve the device performance, TPBI is used as ETL in Device II. The maximum luminance of this device reaches to 2387 cd/m<sup>2</sup> at 8.0 V, and the current efficiency ( $\eta_c$ ) and power efficiency ( $\eta_p$ ) are also slightly higher than those for Device I, as shown in Figure 4. These results can be explained by reduced exciton quenching due to larger distance between excitons and the electrode. Moreover, the deeper HOMO of TPBI 6.2 eV<sup>21</sup> than that of DTPF could also play a role, which could block the holes more effectively and result in a better carrier balance. In Device III, PBD is doped as the ETL, and the maximum luminance goes up to 3110 cd/m<sup>2</sup> at 8.0 V, which is much higher than those in Devices I and II. The  $\eta_c$  and  $\eta_p$  for Device III are 2.55 cd/A and 2.67 lm/W, respectively, which are much better than those of the other two devices (as shown in Figure 4). The excellent performance of Device III can be attributed to the higher electron mobility of PBD ( $1.9 \times 10^{-5}$  cm<sup>2</sup>/(V s))<sup>22</sup> than TPBI ( $1 \times 10^{-6}$  to  $1 \times 10^{-5}$  cm<sup>2</sup>/(V s)).<sup>23</sup> In addition, the deeper HOMO of PBD 6.5 eV,<sup>24</sup> which confines holes in the emitting layer much better than TPBI or DTPF, could also contribute to the better performance.

When the maximum luminance increases from Device I to Device III, the current density decreases from Device I to Device III. This can be understood by the following analysis.

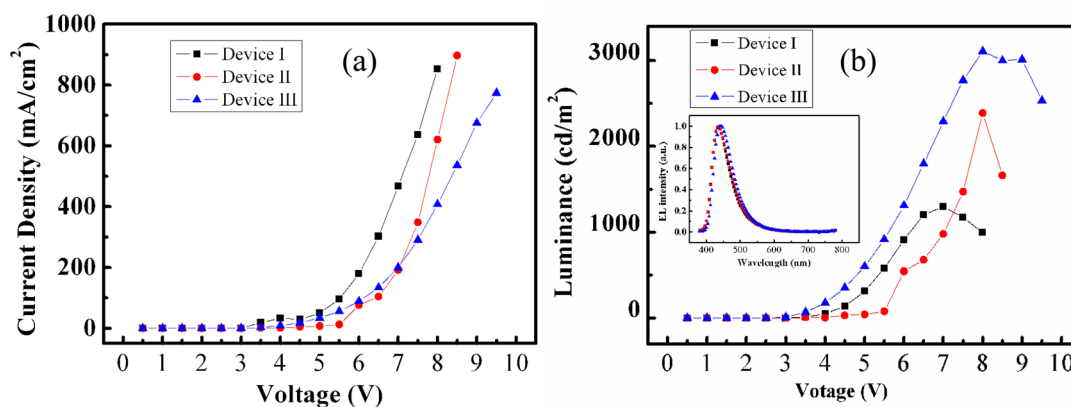


Figure 3. (a) Current density and (b) luminance vs voltage curves for Devices I, II, and III. Inset in b is the electroluminescence spectra emitted from Devices I, II, and III.

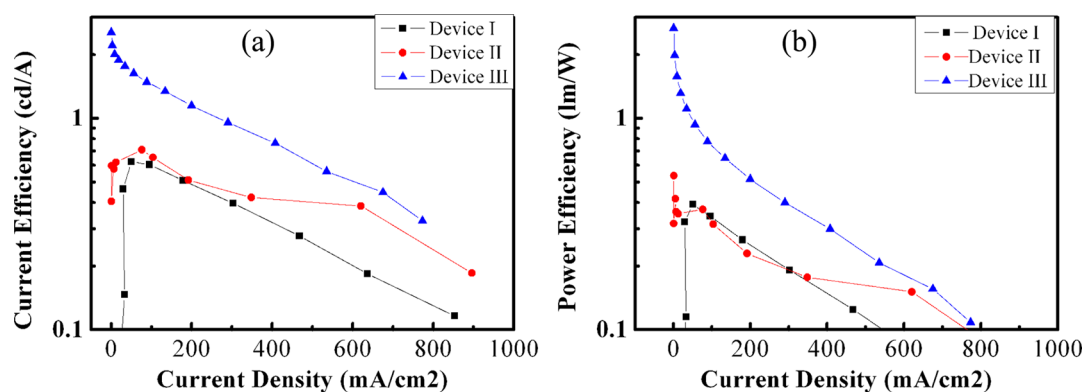


Figure 4. (a) Current efficiency vs current density and (b) power efficiency vs current density.

In OLEDs, current is generated by combinations of holes and electrons with anode and cathode, respectively. The current density ( $J$ ) detected by the instrument is defined by the following formula<sup>25</sup>

$$J = j_h + j_e - j_{\text{com}} \quad (1)$$

Where  $j_h$  is the hole current density and remains the same for the three devices due to the same HTL used in the devices;  $j_e$  is the electron current density.  $j_{\text{com}} = kj_h j_e / e(j_h + j_e)$  is the current density consumed by collisions between holes and electrons, and  $k$  is a constant. Therefore, formula 1 can be rewritten as

$$J = j_h + j_e - kj_h j_e / e(j_h + j_e) \quad (2)$$

For the three devices fabricated in this work,  $j_h$  is kept the same. When the ETL is altered from Device I to Device III, the electron transport ability of the layer is enhanced, resulting in an increased  $j_e$  and  $j_{\text{com}}$ . Consequently the luminance increases from Device I to Device III. However,  $J$  would decrease as formula 2 predicts. Because holes are the majority carriers, when  $j_e$  increases and approaches  $j_h$ , the increased rate of excitons formation results in the increase of the  $\eta_c$  and  $\eta_p$ .

The device performances are summarized in Table 1. All the OLEDs containing DTPF yield an electroluminescence (EL) spectrum with a peak at 436 nm (shown in the inset of Figure 3b). The CIE of them are all very close to the NTSC standard blue of CIE coordinates. A notable deep-blue emission with CIE at (0.16, 0.12) is achieved with a maximum luminance of 3110 cd/m<sup>2</sup> and a high  $\eta_c$  of 2.55 cd/A and  $\eta_p$  of 2.67 lm/W from Device III. This device also exhibits a low turn-on voltage

Table 1. Summary of OLED Performances for Devices I–III.

device	turn-on voltage (V)	max luminance (cd/m <sup>2</sup> )	max $\eta_p$ (lm/W)	max $\eta_c$ (cd/A)	CIE (x, y)
I	3.5	1300	0.39	0.62	0.16, 0.10
II	3.5	2387	0.37	0.71	0.16, 0.09
III	3.0	3110	2.67	2.55	0.16, 0.12

of 3.0 V. The CIE coordinates of the deepest blue reaches (0.16, 0.09) from Device II. These characteristics suggest that DTPF is promising for deep-blue OLED application.

## CONCLUSION

Stable deep-blue light emitting material DTPF with electron transporting property has been developed by balance hole and electron injection/transporting in OLED. High efficiency has been achieved for deep-blue fluorescent OLED. The performance of the devices indicates that deep-blue emitting material DTPF has potential applications for full-color display.

## AUTHOR INFORMATION

### Corresponding Author

\*E-mail: wenfang.sun@ndsu.edu (W.S.); lxxiao@pku.edu.cn (L.X.); qhgong@pku.edu.cn (Q.G.).

### Notes

The authors declare no competing financial interest.

The authors declare no competing financial interest.

## ACKNOWLEDGMENTS

This work was supported by the National Basic Research Program of China (2009CB930504), NSFC (Grants 61177020, 10934001, 60907015, and 11121091), and Beijing Municipal Science and Technology Project (Z101103050410002). W.S. acknowledges the financial support from National Science Foundation (CAREER CHE-0449598).

## REFERENCES

- (1) Tang, C. W.; VanSlyke, S. A. *Appl. Phys. Lett.* **1987**, *51*, 913–915.
- (2) Wu, K. C.; Ku, P. J.; Lin, C. S.; Shih, H. T.; Wu, F. I.; Huang, M. J.; Lin, J. J.; Chen, I. C.; Cheng, C. H. *Adv. Funct. Mater.* **2008**, *18*, 67–75.
- (3) Chien, C. H.; Chen, C. K.; Hsu, F. M.; Shu, C. F.; Chou, P. T.; Lai, C. H. *Adv. Funct. Mater.* **2009**, *19*, 560–566.
- (4) Lee, K. H.; Son, C. S.; Lee, J. Y.; Kang, S.; Yook, K. S.; Jeon, S. O.; Lee, J. Y.; Yoon, S. S. *Eur. J. Org. Chem.* **2011**, 4788–4798.
- (5) D'Andrade, B. W.; Baldo, M. A.; Adachi, C.; Brooks, J.; Thompson, M. E.; Forrest, S. R. *Appl. Phys. Lett.* **2001**, *79*, 1045–1047.
- (6) Kang, D. W.; Kang, J. W.; Park, J. W.; Jung, S. O.; Lee, S. H.; Park, H. D.; Kim, Y. H.; Shin, S. C.; Kim, J. J.; Kwon, S. K. *Adv. Mater.* **2008**, *20*, 2003–2007.
- (7) Rayabarapu, D. K.; Paulose, B. M. J. S.; Duan, J. P.; Cheng, C. H. *Adv. Mater.* **2005**, *17*, 349–353.
- (8) Park, T. J.; Jeon, W. S.; Park, J. J.; Kim, S. Y.; Lee, Y. K.; Jang, J.; Kwon, J. H.; Pode, R. *Appl. Phys. Lett.* **2008**, *92*, 113308–113310.
- (9) Lee, M. T.; Liao, C. H.; Tsai, C. H.; Chen, C. H. *Adv. Mater.* **2005**, *17*, 2493–2497.
- (10) Lin, S. L.; Chan, L. H.; Lee, R. H.; Yen, M. Y.; Kuo, W. J.; Chen, C. T.; Jeng, R. J. *Adv. Mater.* **2008**, *20*, 3947–3952.
- (11) Chien, C. H.; Chen, C. K.; Hsu, F. M.; Shu, C. F.; Chou, P. T.; Lai, C. H. *Adv. Funct. Mater.* **2009**, *19*, 560–566.
- (12) Gao, Z. Q.; Li, Z. H.; Xia, P. F.; Wong, M. S.; Cheah, K. W.; Chen, C. H. *Adv. Funct. Mater.* **2007**, *17*, 3194–3199.
- (13) Cho, I.; Kim, S. H.; Kim, J. H.; Park, S.; Park, S. Y. *J. Mater. Chem.* **2012**, *22*, 123–129.
- (14) Kim, Y. H.; Shin, D. C.; Kim, S. H.; Ko, C. H.; Yu, H. S.; Chae, Y. S.; Kwon, S. K. *Adv. Mater.* **2001**, *13*, 1690–1693.
- (15) Antoniadis, H.; Abkowitz, M. A.; Hsieh, B. R. *Appl. Phys. Lett.* **1994**, *65*, 2030–2032.
- (16) Hancock, J. M.; Gifford, A. P.; Zhu, Y.; Lou, Y.; Jenekhe, S. A. *Chem. Mater.* **2006**, *18*, 4924–4932.
- (17) Kulkarni, A. P.; Kong, X.; Jenekhe, S. A. *Adv. Funct. Mater.* **2006**, *16*, 1057–1066.
- (18) Peng, T.; Ye, K.; Liu, Y.; Wang, L.; Wu, Y.; Wang, Y. *Org. Electron.* **2011**, *12*, 1914–1919.
- (19) Ji, Z.; Li, S.; Li, Y.; Sun, W. *Inorg. Chem.* **2010**, *49*, 1337–1346.
- (20) Xiao, L.; Qi, B.; Xing, X.; Zheng, L.; Kong, S.; Chen, Z.; Qu, B.; Zhang, L.; Ji, Z.; Gong, Q. *J. Mater. Chem.* **2011**, *21*, 19058–19062.
- (21) Gong, S.; Chen, Y.; Luo, J.; Yang, C.; Zhong, C.; Qin, J.; Ma, D. *Adv. Funct. Mater.* **2011**, *21*, 1168–1178.
- (22) Yasuda, T.; Yamaguchi, Y.; Zou, D. C.; Tsutsui, T. *Jpn. J. Appl. Phys., Part 1* **2002**, *41*, 5626–5629.
- (23) Wong, T. C.; Kovac, J.; Lee, C. S.; Hung, L. S.; Lee, S. T. *Chem. Phys. Lett.* **2001**, *334*, 61–64.
- (24) Zhang, F. J.; Zhao, S. L.; Zhao, D. W.; Jiang, W. W.; Li, Y.; Yuan, G. C.; Zhu, H.; Xu, Z. *Phys. Sci.* **2007**, *75*, 407–410.
- (25) Chen, Z. J.; Yu, J. S.; Sakuratani, Y.; Li, M.; Sone, M.; Miyata, S. *J. Appl. Phys.* **2001**, *89*, 7895–7898.